

Bonding in Palladium(II) and Platinum(II) Allyl MeO- and H-MOP Complexes. Subtle Differences via ^{13}C NMR

P. G. Anil Kumar, Pascal Dotta, René Hermatschweiler, and Paul S. Pregosin*

Laboratory of Inorganic Chemistry, ETHZ, 8093 Zürich, Switzerland

Alberto Albinati* and Silvia Rizzato

Department of Structural Chemistry (DCSSI and the Faculty of Pharmacy),
University of Milan, 20133 Milan, Italy

Received December 6, 2004

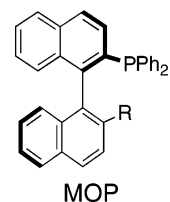
^{13}C NMR studies have shown that in both Pd(II)- and Pt(II)-allyl (modified-MOP) (MOP = (S)-2-diarylphosphino-1,1'-binaphthyl) complexes the substituent on the MOP auxiliary can affect how the naphthyl backbone interacts with a metal center. With the MeO-MOP analogue, the metal binds the carbon in a weak η^1 -fashion, whereas with H-MOP it prefers an η^2 -binding mode. For the Pt complexes, the $^1J(^{195}\text{Pt},^{13}\text{C})$ values proved to be diagnostic tools. Both modes of bonding afford relatively weak bonds to the metal. Modifying the MOP ligand structure from a PPh_2 to a $\text{P}(3,5\text{-di-}t\text{-butylphenyl})_2$ analogue can markedly affect the bond distances within the coordination sphere, as indicated by the X-ray structural data for $\text{PdCl}(\eta^3\text{-C}_3\text{H}_5)(\text{modified-MOP})$. 2-D NMR exchange spectroscopy can be used to recognize and distinguish between the two most common types of $\eta^3\text{-}\eta^1\text{-}\eta^3$ isomerization process, i.e., rotation around the allyl C–C bond versus rotation around the allyl M–C bond. For the complex $\text{PdCl}(\eta^3\text{-C}_3\text{H}_5)(\text{H-MOP})$, the fastest isomerization process involves rotation around the allyl C–C bond.

Introduction

The subject of palladium-catalyzed reactions involving allylic substrates continues to be of growing interest.^{1–5} Several reactions, e.g., allylic alkylation, involve the generation of allyl intermediates, which have been isolated and studied^{1–4} via X-ray diffraction and NMR measurements.

Studies on the use of chiral monodentate phosphine ligands^{6–11} in homogeneous catalysis are increasing. The

MOP ligands, introduced by Hayashi^{6–9} in connection with the allylic alkylation⁷ and hydrosilylation⁶ reactions, represent one of the more successful classes in this area. The MAP ligand, a variation on MOP, with $\text{R} = \text{NMe}_2$, has also been extensively studied.¹⁰



There is some question as to whether these MOP ligands are always complexed to the metal in a monodentate fashion. Kocovsky and co-workers have suggested^{10e} that the complex $[\text{Pd}(\eta^3\text{-C}_3\text{H}_5)(\text{MeO-MOP})]\text{-OTf}$ contains an η^2 -coordinated olefin in which the two Pd–C olefinic distances were observed to be 2.34 and

(1) (a) Helmchen, G.; Ernst, M.; Paradies, G. *Pure Appl. Chem.* **2004**, *76*, 495–506. (b) Kollmar, M.; Helmchen, G. *Organometallics* **2002**, *21*, 4771–4775. (c) Helmchen, G. *J. Organomet. Chem.* **1999**, *576*, 203–214.

(2) Johannsen, M.; Jorgensen, K. A. *Chem. Rev.* **1998**, *98*, 1689–1708.

(3) Trost, B. M.; Crawley, M. L. *Chem. Rev.* **2003**, *103*, 2921–2943. Trost, B. M.; van Vranken, D. L. *Chem. Rev.* **1996**, *96*, 395.

(4) Reiser, O. *Angew. Chem.* **1993**, *105*, 576.

(5) Tye, H. *J. Chem. Soc., Perkin Trans. 1* **2000**, 275–298. Tietze, L. F.; Ila, H.; Bell, H. P. *Chem. Rev.* **2004**, *104*, 3453–3516.

(6) Hayashi, T.; Kawatsura, M.; Uozumi, Y. *J. Am. Chem. Soc.* **1998**, *120*, 1681–1687. Hayashi, T. *J. Organomet. Chem.* **1999**, *576*, 195–202. Hayashi, T. *J. Synth. Org. Chem. Jpn.* **1994**, *52*, 900–911. Shimada, T.; Mukaide, K.; Shinohara, A.; Han, J. W.; Hayashi, T. *J. Am. Chem. Soc.* **2002**, *124*, 1584–1585. Hayashi, T.; Han, J. S.; Takeda, A.; Tang, J.; Nohmi, K.; Mukaide, K.; Tsuji, H.; Uozumi, Y. *Adv. Synth. Catal.* **2001**, *343*, 279–283. Hayashi, T.; Hirate, S.; Kitayama, K.; Tsuji, H.; Torii, A.; Uozumi, Y. *J. Org. Chem.* **2001**, *66*, 1441–1449.

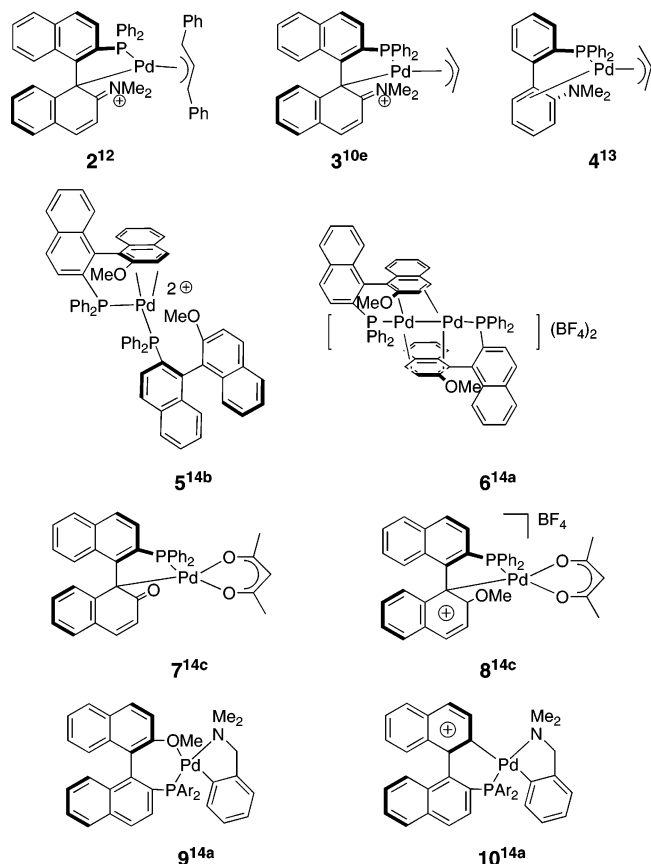
(7) Hayashi, T.; Hirate, S.; Kitayama, K.; Tsuji, H.; Torii, A.; Uozumi, Y. *Chem. Lett.* **2000**, 1272–1273. Uozumi, Y.; Danjo, H.; Hayashi, T. *Tetrahedron Lett.* **1998**, *39*, 8303–8306. Hayashi, T. *Acta Chem. Scand.* **1996**, *50*, 259–266. Uozumi, Y.; Kitayama, K.; Hayashi, T.; Kazunori, K.; Yanagi, K.; Fukuyo, E. *Bull. Chem. Soc. Jpn.* **1995**, *68*, 713–722. Uozumi, Y.; Kitayama, K.; Hayashi, T. *Tetrahedron Asym.* **1993**, *4*, 2419–2422.

(8) Hayashi, T.; Iwamura, H.; Naito, M.; Matsumoto, Y.; Uozumi, Y.; Miki, M.; Yanagi, K. *J. Am. Chem. Soc.* **1994**, *116*, 775–776.

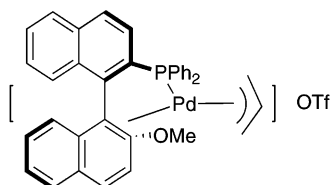
(9) Hayashi, T. *Acc. Chem. Res.* **2000**, *33*, 354–362.

(10) (a) Gouriou, L.; Lloyd-Jones, G. C.; Vyskocil, T.; Kocovsky, P. *J. Organomet. Chem.* **2003**, *687*, 525–537. (b) Kocovsky, P.; Vyskocil, S.; Smrcina, M. *Chem. Rev.* **2003**, *103*, 3213–3245. (c) Fairlamb, I. J. S.; Lloyd-Jones, G. C.; Stepan, V.; Kocovsky, P. *Chem. Eur. J.* **2002**, *8*, 4443–4453. (d) Lloyd-Jones, G. C.; Stephen, S. C.; Murray, M.; Butts, C. P.; Vyskocil, S.; Kocovsky, P. *Chem. Eur. J.* **2000**, *6*, 4348–4357. (e) Kocovsky, P.; Vyskocil, S.; Cisarova, I.; Sejbál, J.; Tislerova, I.; Smrcina, M.; Lloyd-Jones, G. C.; Stephen, S. C.; Butts, C. P.; Murray, M.; Langer, V. *J. Am. Chem. Soc.* **1999**, *121*, 7714–7715. (f) Kocovsky, P.; Malkov, A. V.; Vyskocil, S.; Lloyd-Jones, G. C. *Pure Appl. Chem.* **1999**, *71*, 1425–1433. (g) Vyskocil, S.; Smrcina, M.; Kocovsky, P. *Tetrahedron Lett.* **1998**, *39*, 9289–9292. (h) Vyskocil, S.; Smrcina, M.; Hanus, V.; Polasek, M.; Kocovsky, P. *J. Org. Chem.* **1998**, *63*, 7738–7748.

(11) Feringa, B. L. *Acc. Chem. Res.* **2000**, *33*, 346.

Scheme 1. Different Bonding Modes Exhibited by the MOP Type Complexes

2.47 Å. Subsequently, several groups^{12–14} have shown that these and related monodentate ligands can bind in several ways as indicated in Scheme 1.



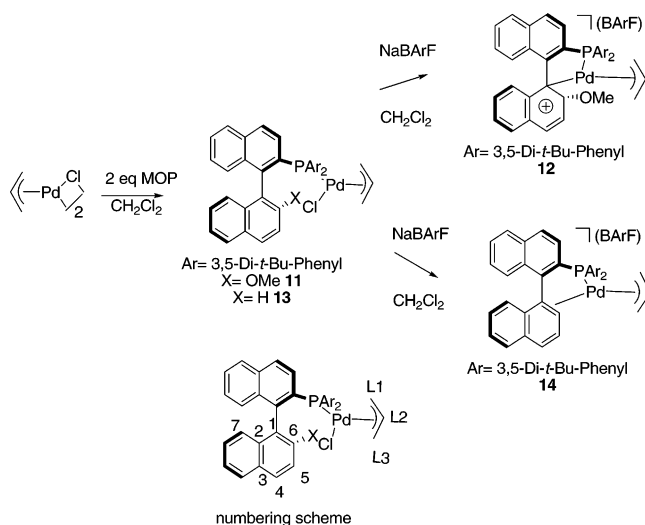
$[\text{Pd}(\eta^3\text{-C}_3\text{H}_5)(\text{MeO-MOP})]\text{OTf}$, as postulated by Kocovsky^{10e}

Scheme 1 shows that differing MOP ligands can function as a chelating P, C σ -donor (complexes **2**, **3**, **7**, **8**, and **10**) or as a phosphine, π -olefin chelate (compounds **5** and **6**) and, reasonably enough, as a P, O chelate via the O atom of the methoxy group, as in **9**. It was found that more than one naphthyl double bond can be involved, as indicated in **5** and **6**. All of these complexes have been characterized via X-ray diffraction and/or multinuclear NMR studies. Given our long-standing interest in π -allyl chemistry,¹⁵ we considered that the description of the $[\text{Pd}(\eta^3\text{-C}_3\text{H}_5)(\text{MeO-MOP})]^+$ cation was still somewhat ambiguous. We report here

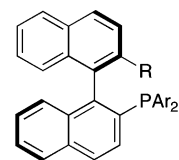
(12) Wang, X. P.; Li, X.; Sun, J.; Ding, K. *Organometallics* **2003**, *22*, 1856–1862.

(13) Faller, J. W.; Sarantopoulos, N. *Organometallics* **2004**, *23*, 2008–2014.

(14) (a) Dotta, P.; Kumar, P. G. A.; Pregosin, P. S.; Albinati, A.; Rizzato, S. *Organometallics* **2004**, *23*, 4247–4254. (b) Dotta, P.; Kumar, P. G. A.; Pregosin, P. S.; Albinati, A. *Helv. Chim. Acta* **2004**, *87*, 272–278. (c) Dotta, P.; Kumar, P. G. A.; Pregosin, P. S.; Albinati, A.; Rizzato, S. *Organometallics* **2003**, *22*, 5345–5349.

Scheme 2. Syntheses of Complexes 11–14

the synthesis of a few cationic Pd(II)- and Pt(II)-MOP allyl complexes containing the modified MOP ligands **1a** and **1b** and their characterization in solution by NMR studies. Several of these complexes display unexpected bonding characteristics.



1a, R = MeO, **1b**, R = H
Ar = 3,5-di-*t*-butylphenyl

Results and Discussion

NMR Studies on $[\text{Pd}(\eta^3\text{-C}_3\text{H}_5)(\text{MOP})]$ Complexes. The syntheses of the Pd-allyl MOP complexes were carried out via the bridge-splitting reactions on the dinuclear complexes $[\text{PdCl}(\eta^3\text{-C}_3\text{H}_5)]_2$ with 2 equiv of **1a** or **1b** to afford **11** and **13** (see Scheme 2). Extraction of the chloride using NaBARF in CH_2Cl_2 solution leads to the cationic complexes $[\text{Pd}(\eta^3\text{-C}_3\text{H}_5)(\text{1a})]\text{BARF}$, **12**, and $[\text{Pd}(\eta^3\text{-C}_3\text{H}_5)(\text{1b})]\text{BARF}$, **14**. The 3,5-di-*tert*-butyl phosphine derivatives were used, as they (a) were available from previous catalytic studies^{14a} and (b) reduced the complexity of the aromatic region of the proton spectra, thereby simplifying the assignment of a number of naphthyl backbone protons.

The various ^1H resonances were assigned via ^1H -COSY and ^{31}P , ^1H correlations as reported previously.¹⁵ One-bond and long-range ^{13}C , ^1H correlations on the

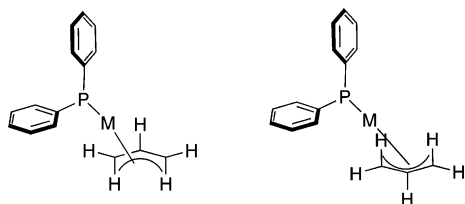
(15) (a) Albinati, A.; Kunz, R. W.; Ammann, C.; Pregosin, P. S. *Organometallics* **1991**, *10*, 1800–1806. (b) Ammann, C. J.; Pregosin, P. S.; Ruegger, H.; Albinati, A.; Lianza, F.; Kunz, R. W. *J. Organomet. Chem.* **1992**, *423*, 415–430. (c) Pregosin, P. S.; Ruegger, H.; Salzmänn, R.; Albinati, A.; Lianza, F.; Kunz, R. W. *Organometallics* **1994**, *13*, 83–90. (d) Breutel, C.; Pregosin, P. S.; Salzmänn, R.; Togni, A. *J. Am. Chem. Soc.* **1994**, *116*, 4067. (e) Pregosin, P. S.; Ruegger, H.; Salzmänn, R.; Albinati, A.; Lianza, F.; Kunz, R. W. *Organometallics* **1994**, *13*, 5040–5048. (f) Abbenhuis, H. C. L.; Burckhardt, U.; Gramlich, V.; Köllner, C.; Pregosin, P. S.; Salzmänn, R.; Togni, A. *Organometallics* **1995**, *14*, 759–766. (g) Pregosin, P. S.; Salzmänn, R.; Togni, A. *Organometallics* **1995**, *14*, 842. (h) Barbaro, P.; Pregosin, P. S.; Salzmänn, R.; Albinati, A.; Kunz, R. W. *Organometallics* **1995**, *14*, 5160–5170. (i) Kositzyna, N.; Antipin, M.; Lyssenko, K.; Pregosin, P. S.; Trabesinger, G. *Inorg. Chim. Acta* **1996**, *250*, 335. (j) Pregosin, P. S.; Salzmänn, R. *Coord. Chem. Rev.* **1996**, *155*, 35–68.

Table 1. ^{13}C Chemical Shifts (in ppm) for the Complexes 11–14

position	11 ^a	12 ^b	13 ^c	14 ^a
	major/minor	major/minor	major	major/minor
1	120.4/120.0	103.2/103.1	136.8	129.2/130.7
2	135.7/134.8	133.1/132.2	133.7	134.1/134.1
3	128.4/128.5	129.4/129.1	133.3	133.9/133.6
4	129.3/129.9	135.0/135.0	128.1	129.4/129.5
5	114.9/114.6	116.1/115.5	126.5	131.1/131.1
6	156.2/156.1	155.3/156.4	131.1	107.4/106.4
OCH ₃	56.6/56.3	57.9/58.8		
L3	80.3/79.3	100.8/100.3	79.0	99.3/100.3
L2	117.1/117.6	121.8/121.5	116.0	122.7/120.5
L1	66.2/60.4	56.5/56.8	61.3	61.5/58.9

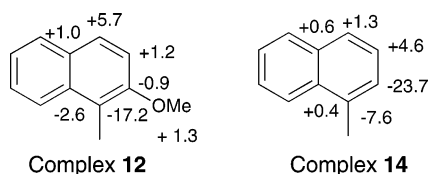
^a Two isomers (major/minor) observed at 273 K. ^b223 K. ^c253 K, for the major isomer (500 MHz, CD₂Cl₂).

isolated allyl complexes were used to locate the key naphthyl backbone carbon resonances via the assigned protons, and selected ^{13}C NMR results for these complexes are shown in Table 1. Note that the allyl groups can be either *exo* or *endo* with respect to the phosphine, with the result that solutions of 11–14 each contain two diastereomers. The carbon chemical shifts were as-



signed for both isomers in 11, 12, and 14, whereas for 13 only the major isomer was assigned. Since there is not much difference in the chemical shifts between these two different allyl isomers, only the data for the major component will be discussed.

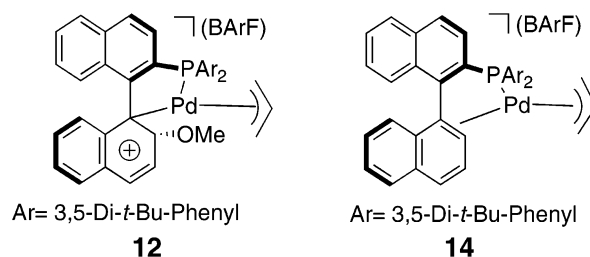
The fragments below show the ^{13}C coordination chemical shifts for the complexes 12 and 14.



The chemical shift for the *ipso* carbon, C-1 in 12, $\delta = 103.2$, has shifted to lower frequency by ca. 17 ppm compared to the neutral chloro complex, 11. Interestingly, there is no significant change in the ^{13}C chemical shift for the MeO-substituted carbon C-6, $\delta = 155.3$. Moreover, the relative changes in the adjacent carbons C-4 and C-5 are modest, so that there is no reason to believe that these atoms are involved in further bonding. The three allyl ^{13}C positions are rather normal with those *pseudo-trans* to phosphorus found at higher frequency relative to those that are *pseudo-trans* to the new bond.¹⁶ Interestingly, the allyl carbon *pseudo-trans* to the P-donor shifts markedly to higher frequency on going from the chloro complex to the cationic complex.

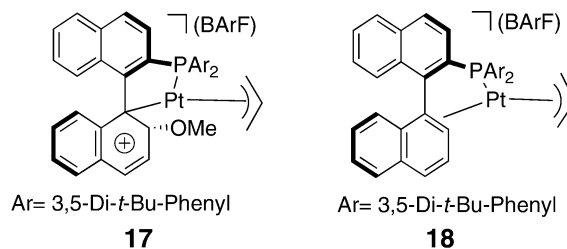
(16) (a) Akermark, B.; Krakenberger, B.; S., H.; Vitagliano, A. *Organometallics* **1987**, *6*, 620. (b) Malet, R.; Moreno-Manas, M.; Pajuelo, F.; Parella, T.; Pleixats, R.; Moreno-Manas, M. *Magn. Reson. Chem.* **1997**, *35*, 227–236.

Our observed ^{13}C chemical shifts for carbons C-1 and C-6 are in agreement with those reported by Kocovsky et al., who find C-1 and C-6 to be at ca. 105 and 157 ppm, respectively. On the basis of these data, the authors suggested that the Pd cation was, partially, bound to the MOP in an η^2 -fashion. We believe that these ^{13}C data for 12 are more consistent with a weak η^1 -bonding mode and suggest that their X-ray data, 2.34 and 2.47 Å for the Pd–C(1) and Pd–C(6) distances, respectively, are consistent with this proposal. The 2.47 Å value is too long for a Pd– η^2 -olefin interaction, whereas the 2.34 Å value is consistent with the η^1 -bonding mode found in 7 and 8.^{14c}



In contrast to 12, the H-MOP complex, 14, shows modest coordination chemical shifts for *both* carbons, ca. 8 ppm for C-1, $\delta = 129.2$, and ca. 24 ppm for C-6, $\delta = 107.4$. Note that, now, C-6, $\delta = 107.4$, and not C-1 has the lowest frequency. We believe these ^{13}C NMR data to be consistent with a weak, polarized complexed π -bond.

NMR Studies on Pt-MOP Complexes. To strengthen our arguments, we prepared related Pt-allyl complexes using the same procedure as described for the Pd analogues. Specifically, the cationic BARF complexes, 17 and 18, were prepared from the neutral PtCl-



(η^3 -allyl)(1a or 1b), 15 and 16, by extraction of chloride with Na(BARF). These Pt derivatives are advantageous in that they provide the coupling constants $^1J(^{195}\text{Pt}, ^{13}\text{C})$. The η^3 -[CH₂C(CH₃)CH₂] allyl fragment was chosen, as this simplifies the allyl spin system and hence makes the Pt–C couplings easier to identify.

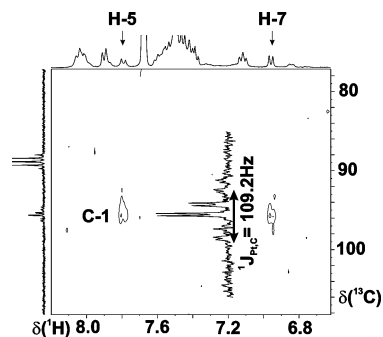
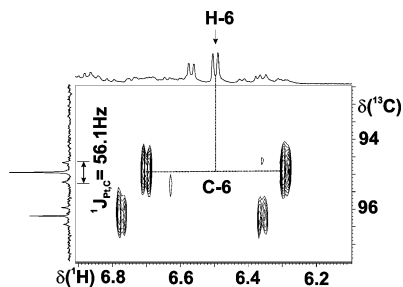
Table 2 gives the ^{13}C chemical shifts for the key carbons in 17 and 18. For the MeO-MOP analogue 17, the signal for C-1 is found at 96.1 ppm and that for C-6 at 152.2 ppm. These chemical shifts are similar to those found in 12. The values $^1J(^{195}\text{Pt}, ^{13}\text{C}-1) = 109.2$ Hz and $^1J(^{195}\text{Pt}, ^{13}\text{C}-6) = 15.3$ Hz are (a) quite different and (b) relatively small. Figure 1 shows the long-range correlation of protons H-5 and H-7 to C-1. Typical σ -bonded ligands, e.g., a Pt–CH₃ interaction, afford $^1J(^{195}\text{Pt}, ^{13}\text{C})$ values in the region of 350–700 Hz,¹⁷ so that the 15.3 Hz value seems more suggestive of a two-bond than a

(17) Mann, B. E.; Taylor, B. F. *^{13}C NMR Data for Organometallic Compounds*; Academic Press: London, 1981.

Table 2. ^{13}C Chemical Shifts (in ppm) for **17** and **18**

position	17 ^a		18 ^b	
	major	minor	major	minor
1	96.1	95.8	116.1	118.7
2	137.4	137.3	132.6	132.0
3	128.0	127.2	132.8	132.2
4	136.0	137.0	129.9	129.7
5	117.7	116.3	131.9	132.5
6	152.2	156.0	95.0	96.1
OCH ₃	57.2	57.3		
L3	89.0	89.5	89.4	92.4
L2	23.9	22.7	24.2	23.0
L1	46.8	45.5	54.5	49.4

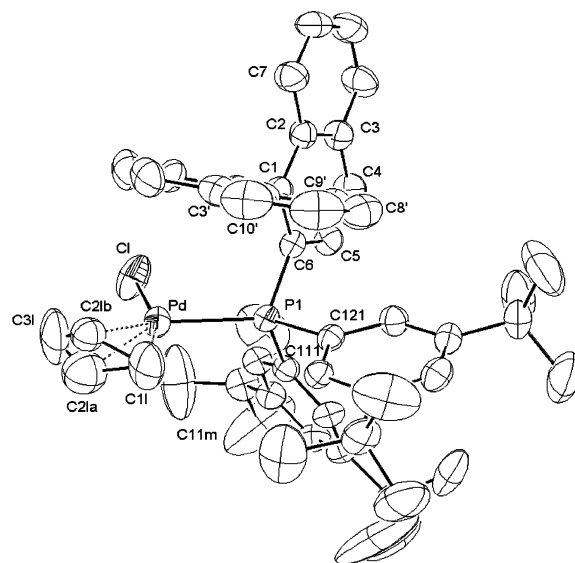
^a **17**: $^1J_{\text{Pt,C}} = 109.2$ (C1), $^1J_{\text{Pt,C}} = 15.3$ (C6). ^b **18**: $^1J_{\text{Pt,C}} = 89.0$ (C1), $^1J_{\text{Pt,C}} = 56.1$ (C6) (400 MHz, CD₂Cl₂).

**Figure 1.** ^{13}C - ^1H HMBC NMR spectrum showing the contacts from H-5 and H-7 to the ipso carbon C-1 in complex **12**.**Figure 2.** One-bond ^{13}C - ^1H correlation for the carbon C-6 in complex **14** showing the carbon signals for the two isomers together with their ^{195}Pt satellites.

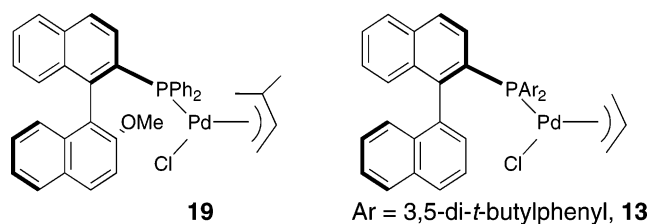
one-bond interaction. Given that our observed $^1J_{(^{195}\text{Pt},^{13}\text{C}-1)}$ in **17** of 109.2 Hz is small (compared to 350–700 Hz), the Pt–C bond in complex **17** must be rather weak. It would seem that the MeO-MOP auxiliary in both the Pd- and Pt-allyl complexes prefers a σ -coordination mode to the *ipso* carbon of the backbone, albeit a weak σ -bond.

For the H-MOP complex **18**, the ^{13}C chemical shifts for C-1 and C-6 are 116.1 and 95.0 ppm, respectively, which are, again, similar to those observed in complex **14**. Figure 2 shows a section of the one-bond ^{13}C , ^1H correlation indicating the carbons with ^{195}Pt -satellites from two different allyl isomers. Carbon C-6 now possesses the lowest resonance frequency. The Pt–C coupling constants, $^1J_{(^{195}\text{Pt},^{13}\text{C}-1)} = 89.0$ Hz and $^1J_{(^{195}\text{Pt},^{13}\text{C}-6)} = 56.1$ Hz, are relatively small, but of a similar size, and suggest a weak π -bond. Typical $^1J_{(^{195}\text{Pt},^{13}\text{C})}$ values in platinum olefin complexes, e.g., $\text{K}[\text{PtCl}_3(\text{C}_2\text{H}_4)]$, are on the order of 150 Hz.¹⁷

X-ray Structure of 13. In contrast to the extensive literature for chiral bidentate ligands, the configuration

**Figure 3.** ORTEP view of **13**. Ellipsoids drawn at 50% probability.

at phosphorus for monodentate ligands such as MOP is not well known. Kocovsky has reported the structure of $[\text{Pd}(\eta^3\text{-C}_3\text{H}_5)(\text{MeO-MOP})]\text{OTf}$, as well as the structures for several “Pd(MAP)” complexes.^{9e} Hayashi has determined the structure of $\text{PdCl}(\eta^3\text{-CH}_2\text{CHC}(\text{Me})_2)(\text{MeO-MOP})$, **19**.⁸



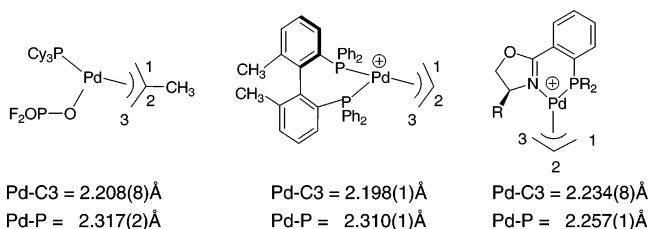
Our modified MOP ligands contain 3,5-di-*tert*-butylphenyl groups, which may affect how the various ligands bond to palladium. Consequently, we have determined the structure of one of our precursors, **13**, and Figure 3 shows a view of this molecule. Selected bond angles and bond distances are given in Table 3. The immediate coordination sphere consists of the three allyl carbon atoms, the MOP P-donor, and the chloride ligand. As reported for **19**, one of the two naphthyl rings is placed over the plane defined by the Pd, P, and Cl atoms, in a pseudo-fifth coordination position. Clearly, after the chloride abstraction reaction, the naphthyl moiety is well placed with respect to a possible interaction with the palladium center. The disorder found for the allyl ligand is a reflection of the two possible diastereomers arising from the position of the allyl ligand.

Two of the Pd–C allyl bond lengths, Pd–C1L and Pd–C2L, are routine^{18a} and are similar to those reported by Kocovsky and Hayashi. However, the bond length Pd–C3L, for the allyl carbon pseudo-*trans* to the P atom, is somewhat short, 2.186(4) Å. The P-donor is

(18) (a) Orpen, A. G.; Brammer, L.; Allen, F. H.; Kennard, O.; Watson, D. G.; Taylor, R. *J. Chem. Soc., Dalton Trans.* **1989**, S1–S83. (b) Farrar, D. H.; Payne, N. C. *J. Am. Chem. Soc.* **1985**, *107*, 2054–2058.

Table 3. Selected Bond Lengths (Å), Bond Angles (deg), and Torsion Angles (deg) for 13

Pd–P(1)	2.328(1)
Pd–Cl	2.369(1)
Pd–C(1L)	2.136(4)
Pd–C(2LB)	2.169(8)
Pd–C(3L)	2.186(4)
P(1)–C(6)	1.835(3)
P(1)–C(121)	1.827(3)
P(1)–C(111)	1.842(3)
C(1L)–C(2LB)	1.367(8)
C(3L)–C(2LB)	1.326(9)
C(1)–C(1')	1.510(4)
<C–C> _{naphth}	1.40(3)
P(1)–Pd–Cl	93.19(4)
C(1L)–Pd–C(3L)	67.7(2)
P(1)–Pd–C(1L)	105.0(1)
P(1)–Pd–C(3L)	171.9(2)
Cl–Pd–C(1L)	161.8(1)
Cl–Pd–C(3L)	94.1(2)
C(1L)–C(2LB)–C(3L)	126.6(8)
Pd–P(1)–C(6)	113.1(1)
C(6)–P(1)–C(111)	104.3(1)
C(6)–P(1)–C(121)	101.1(2)
C(111)–P(1)–C(6)–C(5)	10.7(3)
C(121)–P(1)–C(6)–C(5)	93.9(3)
C(6)–C(1)–C(1')–C(6')	94.4(4)

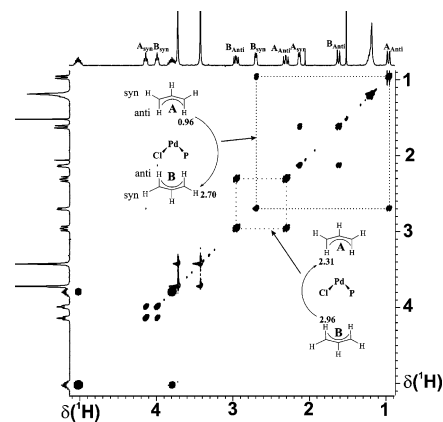
Scheme 3. Model PCy₃,³² Biphenp,³³ and Oxazoline³⁴ Pd Complexes

expected to have a relatively strong *trans* influence, and, consequently, values on the order of ca. 2.2 Å^{18b} for this Pd–C separation would have been normal. Scheme 3 shows Pd–C and Pd–P bond lengths from selected model complexes.

Further, in **13**, the observed distances Pd–P, 2.328(1) Å, and Pd–Cl, 2.369(1) Å, are relatively long. The corresponding values in the MeO–MOP complex, **19**, are 2.310(1) and 2.304(4) Å. The model complexes in Scheme 3 also indicate that a Pd–P separation of 2.31 Å, or less, might be expected. Perhaps there is some steric crowding induced by the presence of the *tert*-butyl groups. In agreement with steric congestion, we note the slightly large P–Pd–Cl angle of ca. 93° (90° in **19**). We also note that there is a short contact, ca. 2.6 Å, between the hydrogen on C122 (an *ortho* carbon of one P-aryl) and the allyl carbon C1L. It appears that the presence of the *tert*-butyl phenyl groups, within this fairly simple molecule, can markedly affect the observed bond lengths. This is surprising, but not completely unexpected.¹⁹

Interestingly, our ¹³C studies on the terminal allyl carbons of complex **13** do not reflect what we find in the solid state. The carbon pseudo-*trans* to the P-donor, at 79.0 ppm, is found at much higher frequency than that located pseudo-*trans* to chloride, 61.3 ppm. For a related PPh₃ complex, reported by Akermark,^{16a} the two

(19) Dotta, P.; Kumar, P. G. A.; Pregosin, P. S. *Magn. Reson. Chem.* **2002**, *40*, 653–658.

**Figure 4.** Exchange spectrum for [PdCl(η^3 -C₃H₅)(MeO-MOP)] at 273 K with a mixing time of 50 ms.

terminal allyl carbon resonances are found at 78.0 and 61.6 ppm, respectively; that is, there is little difference between these two.

Dynamic Studies on [PdCl(η^3 -C₃H₅)(MeO-MOP)]. It is well known^{15j,20–24} that allyl complexes are often found to be dynamic on the NMR time scale, and this is usually associated with η^3 – η^1 – η^3 isomerization processes.

The ¹H spectrum of the neutral [PdCl(η^3 -C₃H₅)(MeO-MOP)] complex (without *tert*-butyl groups, as these obscure several important allyl resonances) revealed a series of broad signals for the allyl protons. On cooling to 273 K, these resonances sharpen sufficiently to reveal proton–proton and proton–phosphorus spin–spin interactions. Figure 4 shows the phase-sensitive ¹H-NOESY at 273 K, with a mixing time of 50 ms. The exchange cross-peaks connecting the two methoxy methylene resonances (and those stemming from the central allyl protons, CH₂CHCH₂) clearly indicate the exchange. These exchange measurements were repeated using several mixing times (50, 100, 200, and 600 ms), thereby allowing an estimate of the exchange rate: 2.2 s^{–1}(1) (*T*₁ relaxation times were around 500 ms). Further, with a 50 ms mixing time, one finds selective *syn/anti* exchange for the allyl methylene proton pairs *trans* to the chloride ligand (see Figure 4). The *syn* and *anti* allyl methylene protons *trans* to phosphorus do not exchange positions on going from one isomer to the other. It is well known that the η^3 – η^1 isomerization mechanism can

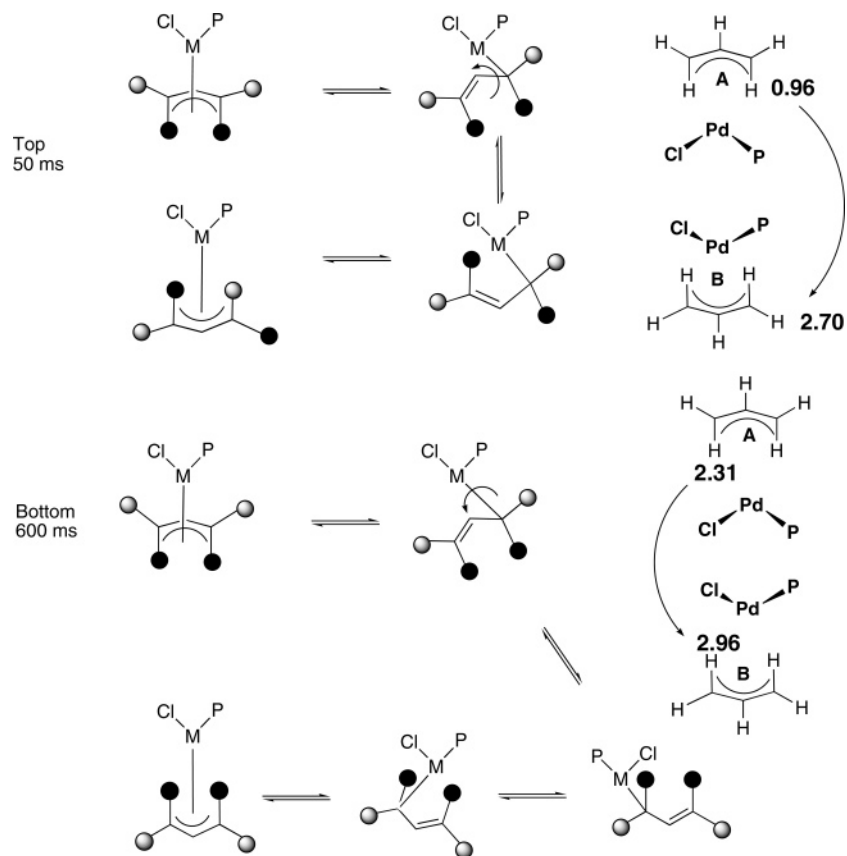
(20) Faller, J. W. *Determination of Organic Structures by Physical Methods*; Academic Press: New York, 1973; Vol. 5. Faller, J. W.; Stokes-Huby, H. L.; Albrizzio, M. A. *Helv. Chim. Acta* **2001**, *84*, 3031–3042. Faller, J. W.; Sarantopoulos, N. *Organometallics* **2004**, *23*, 2179–2185.

(21) Cesarotti, E.; Grassi, M.; Prati, L.; Demartin, F.; Grassi, M. *J. Organomet. Chem.* **1989**, *370*, 407–419. Cesarotti, E.; Grassi, M.; Prati, L.; Demartin, F. *J. Chem. Soc., Dalton Trans.* **1991**, 2073.

(22) (a) Gogoll, A.; Ornebro, J.; Grennberg, H.; Bäckvall, J. E. *J. Am. Chem. Soc.* **1994**, *116*, 3631. (b) Fernandez-Galan, R.; Jalón, F. A.; Manzano, B. R.; Rodriguez de la Fuente, J.; Vreahami, M.; Jedlicka, B.; Weissensteiner, W.; Jögl, G. *Organometallics* **1997**, *16*, 3758–3768. (c) Mandal, S. K.; Gowda, G. A. N.; Krishnamurthy, S. S.; Zheng, C.; Li, S. J.; Hosmane, N. S. *Eur. J. Inorg. Chem.* **2002**, 2047–2056.

(23) Crociani, B.; Antonaroli, S.; Bandoli, G.; Canovese, L.; Visentin, F.; Uguagliati, P. *Organometallics* **1999**, *18*, 1137–1147. Crociani, B.; Benetollo, F.; Bertani, R.; Bombieri, G.; Meneghetti, F.; Zanutto, L. *J. Organomet. Chem.* **2000**, *605*, 28–38.

(24) Sprinz, J.; Kiefer, M.; Helmchen, G.; Reggelin, M.; Huttner, G.; Zsolnai, L. *Tetrahedron Lett.* **1994**, *35*, 1523–1526. Steinhagen, H.; Reggelin, M.; Helmchen, G. *Angew. Chem., Int. Ed. Engl.* **1997**, *36*, 2108–2110.

Scheme 4. Isomerization Mechanisms for the Allyl Fragment in the $[\text{PdCl}(\eta^3\text{-C}_3\text{H}_5)(\text{MeO-MOP})]$ Complex

be under either electronic or steric control, and examples of both have been reported.^{15j} Apparently, in **13**, the former dominates,^{22b,c} in that the allyl opens *trans* to the P-donor to afford a Pd–C σ -bond *trans* to Cl. Rotation around the $\text{sp}^3\text{-sp}^2$ C–C bond exchanges the *syn* and *anti* protons *trans* to chloride ligand, and after $\eta^1\text{-}\eta^3$ isomerization, the process is complete (see Scheme 4, top). These dynamics are in keeping with those reported by Lloyd-Jones^{10d} for a related Pd(MAP) complex.

Interestingly, if one increases the mixing time to 600 ms, i.e., one waits longer, then new cross-peaks are observed in the exchange spectrum at 273 K (see Figure 5). These new exchange peaks can be assigned to an exchange process involving *syn* protons which were in pseudo-*trans* position to the P-donor, but which are now

occupying *syn* positions pseudo-*trans* to the chloride (i.e., no *syn/anti* exchange, but positional exchange). We believe that this slower process arises from *both* isomerization of the “T”-shaped three-coordinate complex and rotation around the M–C bond, as indicated in Scheme 4, bottom. Taken together, these 2-D NMR results represent a rare example of the distinction between these two mechanisms (rotation around the C–C bond versus rotation around the M–C bond) via use of the 2-D exchange mixing time.

Comments. In conclusion, we have shown that in both Pd(II)- and Pt(II)-allyl complexes the substituent R on the MOP auxiliary can affect how the naphthyl backbone interacts with a metal center. With the MeO-MOP ligand, the metal binds the carbon in a weak η^1 -fashion, whereas with H-MOP it prefers an η^2 -binding mode. Both modes of bonding afford relatively weak bonds to the metal. Although the nature of the MOP ligand plays a role in these allyl compounds, Kocovsky and co-workers have correctly recognized—and our various studies¹⁴ on cyclometalated MOP compounds, among others, support this view—that a monodentate description need not be correct for the coordination chemistry of MOP and related ligands. The presence of the 3,5-*tert*-butyl phenyl groups can affect the P-donor capability as indicated by the solid-state structural data for $\text{PdCl}(\eta^3\text{-C}_3\text{H}_5)(\mathbf{1b})$, in which the Pd–P bond is relatively long (and thus one Pd–C(allyl) separation, relatively short). Finally, one can distinguish between two allyl isomerization mechanisms (rotation around the C–C bond versus rotation around the M–C bond) via use of several 2-D mixing times.

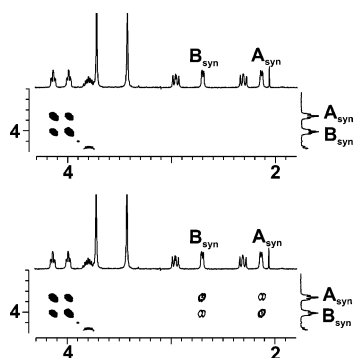


Figure 5. Comparison of sections of the two exchange spectra for the two different mixing times. Note the appearance of new cross-peaks in the lower slice with a 600 ms mixing time.

Table 4. Experimental Data for the X-ray Diffraction Study of 13

formula	C ₅₁ H ₅₄ ClPPd
mol wt	839.76
data coll. T, K	293 (2)
diffractometer	Bruker SMART CCD
cryst syst	orthorhombic
space group (no.)	P2 ₁ 2 ₁ 2 ₁ (19)
a, Å	10.2757(7)
b, Å	20.044(1)
c, Å	22.322(2)
V, Å ³	4597.6(5)
Z	4
ρ _(calcd) , g cm ⁻³	1.213
μ, cm ⁻¹	5.28
radiation	Mo Kα (graphite monochrom., λ = 0.71073 Å)
θ range, deg	2.41 < θ < 27.52
no. data collected	48 277
no. indep data	10 527
no. obsd reflns (n _o)	8033
[F _o ² > 2.0σ(F ²)]	
no. of params refined (n _v)	487
R _{int}	0.0590
R (obsd reflns) ^a	0.0405
R _w ² (obsd reflns) ^b	0.0900
GOF ^c	1.029
absolute struct param (Flack's param)	0.03(2)

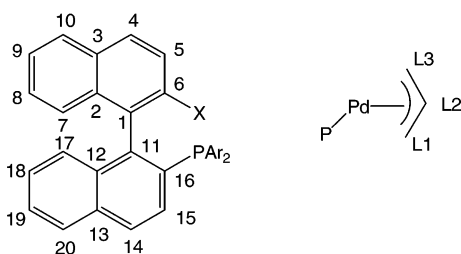
^a $R = \sum(|F_o - (1/k)F_c|)/\sum|F_o|$. ^b $R_w^2 = [\sum w(F_o^2 - (1/k)F_c^2)^2]/\sum w|F_o^2|^2$. ^c GOF = $[\sum w(F_o^2 - (1/k)F_c^2)^2/(n_o - n_v)]^{1/2}$.

Experimental Section

All water- or air-sensitive manipulations were carried out under a nitrogen atmosphere. Pentane and ether were distilled from NaK, THF and toluene from potassium, and CH₂Cl₂ from CaH₂. The MOP ligands were prepared according to literature procedures.

NMR spectra were recorded with Bruker DPX-250, 300, 400, and 500 MHz spectrometers at room temperature unless otherwise noted. Chemical shifts are given in ppm; coupling constants (*J*) in hertz. Elemental analyses and mass spectroscopic studies were performed at ETHZ.

Numbering schemes:



Crystallography. Air-stable, yellow crystals of **13** suitable for X-ray diffraction were obtained by crystallization from dichloromethane/pentane. A prismatic single crystal of the compound was mounted on a glass fiber at a random orientation. A Bruker SMART CCD diffractometer was used for the space group determination and for the data collection. The space group was determined from the systematic absences, while the cell constants were refined at the end of the data collection with the data reduction software SAINT.²⁵ The experimental conditions for the data collection, plus crystallographic and other relevant data, are listed in Table 4 and in the Supporting Information. The collected intensities were corrected for Lorentz and polarization factors²⁵ and empirically for absorption using the SADABS program.²⁶

(25) Bruker AXS, SAINT, Integration Software; Bruker Analytical X-ray Systems: Madison, WI, 1995.

The standard deviations on intensities were calculated in terms of statistics alone. The structure was solved by direct and Fourier methods and refined by full matrix least squares,²⁷ minimizing the function $[\sum w(F_o^2 - (1/k)F_c^2)^2]$ and using anisotropic displacement parameters for all atoms except for the hydrogen atoms. In the difference Fourier maps two orientations for the allyl ligand were identified. Splitting the C2 atom into two positions and refining the result using isotropic temperature factors modeled the positional disorder. Moreover some of the *tert*-butyl groups are disordered, as shown by the values of the ADPs, possibly due to large-amplitude torsional vibrations. No extinction correction was deemed necessary. Upon convergence, the final Fourier difference map showed no significant peaks.

The contribution of the hydrogen atoms, in their calculated position (C–H = 0.95 Å), $B(H) = 1.2 \times B(C_{\text{bonded}})$ (Å²), was included in the refinement using a riding model. Refining the Flack's parameter²⁸ tested the handedness of the structure. The scattering factors used, corrected for the real and imaginary parts of the anomalous dispersion, were taken from the literature.²⁹ All calculations were carried out by using the PC version of the programs WINGX,³⁰ SHELX-97,²⁷ and ORTEP.³¹

Synthesis of PdCl(η³-C₃H₅)(1a**), **11.** To a mixture of **1a** (100 mg, 0.144 mmol) and [Pd(μ-Cl)(η³-C₃H₅)₂] (26.4 mg, 0.072 mmol) was added 3 mL of CH₂Cl₂, and the resulting solution was stirred for 60 min at room temperature. After removal of the solvent, 4 mL of pentane was added to give a clear solution, from which the product precipitated after a few minutes. Yield: 112.9 mg (90%). Anal. Calcd for C₅₂H₆₂OClPd: C, 71.31; H, 7.13. Found: C, 71.43; H, 7.06. ¹H NMR (CD₂Cl₂, 500 MHz, 273 K): major isomer: δ 7.97 (d, ³J_{HH} = 8.1, H-4), 7.72 (d, ³J_{HH} = 8.1, H-10), 7.54 (H-5), 6.93 (d, ³J_{HH} = 8.2, H-7), 4.96 (m, H-L2), 4.05 (t, ³J_{PH} = ³J_{HH} = 7.1, H^{cis}-L3), 3.91 (s, OCH₃), 2.00 (dd, ³J_{PH} = 11.2, ³J_{HH} = 14.1, H^{trans}-L3), 1.57 (H^{cis}-L1), 1.19 (s, C(CH₃)₃, 18 H), 1.16 (s, C(CH₃)₃, 18 H), 0.13 (d, *J* = 12.2, H^{trans}-L1). Minor isomer: δ 7.94 (d, ³J_{HH} = 9.2, H-4), 7.37 (d, ³J_{HH} = 9.7, H-5), 6.96 (H-7), 3.90 (H^{cis}-L3), 3.52 (s, OCH₃), 3.38 (m, H-L2), 2.97 (dd, ³J_{PH} = 8.9, ³J_{HH} = 14.1, H^{trans}-L3), 2.18 (d, ³J_{HH} = 5.9, H^{cis}-L1), 1.47 (d, ³J_{HH} = 12, H^{trans}-L1), 1.21 (s, C(CH₃)₃, 18 H), 1.15 (s, C(CH₃)₃, 18 H). ¹³C NMR (CD₂Cl₂, 125 MHz, 273 K): major isomer: δ 156.2 (C-6), 135.7 (C-2), 129.3 (C-4), 128.4 (C-3), 120.4 (C-1), 117.1 (C-L2), 114.9 (C-5), 80.3 (C-L3), 66.2 (C-L1), 56.6 (OCH₃), 35.2 (C(CH₃)₃), 31.5 (C(CH₃)₃). Minor isomer: δ 156.1 (C-6), 134.8 (C-2), 129.9 (C-4), 128.5 (C-3), 120.0 (C-1), 117.6 (C-L2), 114.6 (C-5), 79.3 (C-L3), 60.4 (C-L1), 56.3 (OCH₃), 35.2 (C(CH₃)₃), 31.5 (C(CH₃)₃). ³¹P NMR (CD₂Cl₂, 202 MHz, 273 K): major isomer: δ 12.6 (s). Minor isomer: δ 16.1 (s). MS(MALDI): 835.2 (M⁺ - C₃H₅, 100%).**

Synthesis of [Pd(η³-C₃H₅)(1a**)](BArF), **12.** Complex **11** (68.9 mg, 0.079 mmol) and NaBArF (69.7 mg, 0.079 mmol) were dissolved in 3 mL of CH₂Cl₂, and the resulting solution was stirred for 30 min at room temperature. The NaCl formed was removed by filtration over Celite and the solvent evaporated in vacuo. Yield: 90 mg (67%). Anal. Calcd for C₈₄H₇₄OBF₂PPd: C, 59.22; H, 4.38. Found: C, 59.40; H, 4.58. ¹H NMR (CD₂Cl₂, 500 MHz, 223 K): major isomer: δ 8.09 (d, ³J_{HH} = 9.2, H-4), 7.81 (d, ³J_{HH} = 9.2, H-5), 7.10 (H-7), 5.60 (m,**

(26) Sheldrick, G. M. SADABS, Program for Absorption Correction; University of Göttingen: Göttingen, Germany, 1996.

(27) Sheldrick, G. M. SHELX-97. *Structure Solution and Refinement Package*; Universität Göttingen, 1997.

(28) Flack, H. D. *Acta Crystallogr.* **1983**, A39, 876.

(29) *International Tables for X-ray Crystallography*; Wilson, A. J. C., Ed.; Kluwer Academic Publisher: Dordrecht, The Netherlands, 1992; Vol. C.

(30) Farrugia, L. J. *J. Appl. Crystallogr.* **1999**, 32, 837.

(31) Farrugia, L. J. *J. Appl. Crystallogr.* **1997**, 30, 565.

(32) Fernandez-Galan, R.; Manzano, B. R.; Otero, A.; Lanfranchi, M.; Pellinghelli. *Inorg. Chem.* **1994**, 33, 2309–2312.

(33) Knierzinger, A.; Scholzer, P. *Helv. Chim. Acta* **1992**, 75, 1211.

(34) Schaffner, S.; Kueller, J. F. K.; Neuburger, M.; Zehnder, M. *Helv. Chim. Acta* **1998**, 81, 1223–1232.

H-L2), 3.71 (s, OCH₃), 3.48 (d, ³J_{HH} = 4.8, H^{cis}-L1), 2.80 (dd, ³J_{PH} = 9.9, ³J_{HH} = 14.6, H^{trans}-L3), 2.62 (bt, H^{cis}-L3), 2.37 (d, ³J_{HH} = 12.2, H^{trans}-L1), 1.18 (s, C(CH₃)₃, 18 H), 1.17 (s, C(CH₃)₃, 18 H). Minor isomer: δ 8.10 (d, ³J_{HH} = 9.2, H-4), 7.91 (d, ³J_{HH} = 9.2, H-5), 5.06 (m, H-L2), 3.86 (dd, ³J_{PH} = 10, ³J_{HH} = 14.8, H^{trans}-L3), 3.79 (s, OCH₃), 3.41 (d, ³J_{HH} = 4.9, H^{cis}-L1), 2.51 (d, ³J_{HH} = 12.3, H^{trans}-L1), 2.13 (bt, H^{cis}-L3), 1.18 (s, C(CH₃)₃, 18 H), 1.16 (s, C(CH₃)₃, 18 H). ¹³C NMR (CD₂Cl₂, 125 MHz, 223 K): major isomer: δ 155.3 (C-6), 135.0 (C-4), 133.1 (C-2), 129.4 (C-3), 124.6 (C-7), 121.8 (C-L2), 116.1 (C-5), 103.2 (C-1), 100.8 (C-L3), 57.9 (OCH₃), 56.5 (C-L1), 35.4 (C(CH₃)₃), 31.4 (C(CH₃)₃). Minor isomer: δ 156.4 (C-6), 135.0 (C-4), 132.2 (C-2), 129.1 (C-3), 124.5 (C-7), 121.5 (C-L2), 115.5 (C-5), 103.1 (C-1), 100.3 (C-L3), 58.0 (OCH₃), 56.8 (C-L1), 35.4 (C(CH₃)₃), 31.4 (C(CH₃)₃). ³¹P NMR (CD₂Cl₂, 202 MHz, 223 K): major isomer: δ 40.6 (s). Minor isomer: δ 40.2 (s). MS(ESI): 839.1 (M⁺ - BARF, 100%).

Synthesis of PdCl(η³-C₃H₅)(1b), 13. To a mixture of **1b** (100 mg, 0.151 mmol) and [Pd(μ-Cl)(η³-C₃H₅)₂] (27.6 mg, 0.075 mmol) was added 3 mL of CH₂Cl₂, and the resulting solution was stirred for 40 min at room temperature. After removal of the solvent, the product was washed with 4 mL of pentane. Yield: 94 mg (74%). Anal. Calcd for C₅₁H₆₀PClPd: C, 72.42; H, 7.15. Found: C, 72.32; H, 7.13. ¹H NMR (CD₂Cl₂, 500 MHz, 253 K): major isomer: δ 7.87 (H-6), 7.83 (d, ³J_{HH} = 8.2, H-4), 7.74 (d, ³J_{HH} = 8.4, H-10), 7.53 (dd, ³J_{HH} = 8.2 und 7.2, H-5), 7.24 (H-9), 6.86 (t, ³J_{HH} = 8.1, H-8), 6.81 (d, ³J_{HH} = 8.7, H-7), 4.86 (m, H-L2), 4.18 (dt, ³J_{HH} = 7.4, ³J_{PH} = 2.1, H^{cis}-L3), 2.86 (dd, ³J_{PH} = 10.2, ³J_{HH} = 13.3, H^{trans}-L3), 2.46 (d, ³J_{HH} = 6.3, H^{cis}-L1), 1.14 (s, C(CH₃)₃, 18 H), 1.10 (s, C(CH₃)₃, 18 H), 0.99 (d, ³J_{HH} = 12.8, H^{trans}-L1). Minor isomer: δ 7.32 (H-5), 7.13 (H-7), 4.56 (m, H-L2), 4.04 (dt, ³J_{HH} = 7.2, ³J_{PH} = 1.6, H^{cis}-L3), 2.72 (d, ³J_{HH} = 6.6, H^{cis}-L1), 2.36 (dd, ³J_{PH} = 9.4, ³J_{HH} = 13.7, H^{trans}-L3), 1.46 (d, ³J_{HH} = 12.0, H^{trans}-L1), 1.15 (s, C(CH₃)₃, 18 H), 1.11 (s, C(CH₃)₃, 18 H). ¹³C NMR (CD₂Cl₂, 125 MHz, 253 K): major isomer: δ 136.8 (C-1), 133.7 (C-2), 133.3 (C-3), 131.1 (C-6), 128.1 (C-4), 128.1 (C-10), 127.5 (C-7), 126.5 (C-5), 126.2 (C-9), 126.1 (C-8), 116.0 (C-L2), 79.0 (C-L3), 61.3 (C-L1), 35.3 (C(CH₃)₃), 35.2 (C(CH₃)₃), 31.4 (C(CH₃)₃). Minor isomer: δ 136.8 (C-1), 117.0 (C-L2), 79.2 (C-L3), 58.5 (C-L1), 35.3 (C(CH₃)₃), 35.2 (C(CH₃)₃), 31.4 (C(CH₃)₃). ³¹P NMR (CD₂Cl₂, 202 MHz, 253 K): major isomer: δ 18.5 (s). Minor isomer: δ 21.5 (s). MS(MALDI): 809 (M⁺ - Cl, 100%), 769 (M⁺ - C₃H₅ - Cl, 60%).

Synthesis of [Pd(η³-C₃H₅)(1b)](BARF), 14. Complex **13** (50.0 mg, 0.059 mmol) and NaBARF (52.4 mg, 0.059 mmol) were dissolved in 3 mL of CH₂Cl₂, and the resulting solution was stirred for 30 min at room temperature. The NaCl formed was removed by filtration over Celite and the solvent evaporated in vacuo. Yield: 74.9 mg (67%). Anal. Calcd for C₈₃H₇₂-BF₂PPd: C, 59.57; H, 4.34. Found: C, 59.60; H, 4.60. ¹H NMR (CD₂Cl₂, 500 MHz, 273 K): major isomer: δ 8.12 (dd, ³J_{HH} = 6.4 and 8.9, H-5), 7.87 (H-4), 7.10 (H-7), 7.02 (d, ³J_{HH} = 6.4, H-6), 5.70 (m, H-L2), 3.90 (bt, H^{cis}-L3), 3.60 (bd, ³J_{HH} = 6.4, H^{cis}-L1), 2.76 (dd, ³J_{PH} = 9.7, ³J_{HH} = 14.8, H^{trans}-L3), 2.63 (d, ³J_{HH} = 12.5, H^{trans}-L1), 1.21 (s, C(CH₃)₃, 36 H). Minor isomer: δ 8.19 (dd, ³J_{HH} = 6.4 und 8.9, H-5), 7.86 (H-4), 7.15 (H-6), 5.01 (m, H-L2), 4.26 (dd, ³J_{PH} = 10, ³J_{HH} = 14.6, H^{trans}-L3), 3.48 (bd, ³J_{HH} = ca. 6.1, H^{cis}-L1), 3.15 (bt, H^{cis}-L3), 2.56 (d, ³J_{HH} = 12.5, H^{trans}-L1), 1.19 (s, C(CH₃)₃, 18 H), 1.15 (s, C(CH₃)₃, 18 H). ¹³C NMR (CD₂Cl₂, 125 MHz, 273 K): major isomer: δ 134.1 (C-2), 133.9 (C-3), 131.1 (C-5), 129.4 (C-4), 129.2 (C-1), 122.7 (C-L2), 107.4 (C-2), 99.3 (C-L3), 61.5 (C-L1), 35.3 (C(CH₃)₃), 31.3 (C(CH₃)₃). Minor isomer: δ 134.1 (C-2), 133.6 (C-3), 131.1 (C-5), 130.7 (C-1), 129.5 (C-4), 120.5 (C-L2), 106.4 (C-2), 100.3 (C-L3), 58.9 (C-L1), 35.3 (C(CH₃)₃), 31.3 (C(CH₃)₃), 31.2 (C(CH₃)₃). ³¹P NMR (CD₂Cl₂, 202 MHz, 273 K): major isomer: δ 36.5 (s). Minor isomer: δ 36.2 (s). MS(ESI): 809.1 (M⁺ - BARF, 100%).

Synthesis of [PtCl(η³-C₃H₄(Me))(1a, Ar = Ph)], 15. To a mixture of the MeO-MOP ligand (115 mg, 0.245 mmol) and

[Pt(μ-Cl)(η³-C₃H₄(Me))]₂ (70 mg, 0.123 mmol) was added 4 mL of CH₂Cl₂, and the resulting solution was stirred for 60 min at room temperature. After removal of the solvent, the product was washed with 4 mL of pentane. Yield: 169 mg (91%). Anal. Calcd for C₃₇ClH₃₂OPPt: C, 58.93; H, 4.28. Found: C, 58.79; H, 4.48. ¹H NMR (CD₂Cl₂, 500 MHz, 298 K): major isomer: δ 7.86 (³J_{HH} = 9.2, H-4), 7.26 (H-5), 3.80 (s, OCH₃), 3.75 (bm, H^{cis}-L3), 1.92 (⁴J_{HH} = 2.4, H^{cis}-L1), 1.88 (³J_{PH} = 10.1, H^{trans}-L3), 1.76 (³J_{PH} = 74.8, CH₃-L2), 0.74 (²J_{PH} = 75.4, ⁴J_{HH} = 2.2, H^{trans}-L1). Minor isomer: δ 7.65 (³J_{HH} = 9.2, H-4), 6.91 (³J_{HH} = 9.2, H-5), 3.97 (bt, H^{cis}-L3), 3.58 (s, OCH₃), 2.65 (m, ³J_{PH} = 9.4, H^{trans}-L3), 2.64 (H^{cis}-L1), 2.05 (³J_{PH} = 71.7, CH₃-L2), 1.99 (H^{trans}-L1). ¹³C NMR (CD₂Cl₂, 125 MHz, 298 K): major isomer: δ 155.6 (C-6), 135.0 (C-2), 129.9 (C-4), 125.0 (C-L2), 119.9 (C-1), 113.8 (C-5), 67.8 (C-L3), 55.8 (OCH₃), 50.8 (C-L1), 23.4 (C(CH₃)-L2). Minor isomer: δ 154.7 (C-6), 134.6 (C-2), 130.9 (C-4), 129.0 (C-3), 125.0 (C-L2), 119.3 (C-1), 112.3 (C-5), 66.9 (C-L3), 55.6 (OCH₃), 49.5 (C-L1), 23.6 (C(CH₃)-L2). ³¹P NMR (CD₂Cl₂, 202 MHz, 298 K): major isomer: δ 20.8 (s, ¹J_{PtP} = 4379). Minor isomer: δ 27.4 (s, ¹J_{PtP} = 4364). ESI: 718.1 (M⁺ - Cl), 694.0, 662.0 (M⁺ - Cl, - C₄H₇), 633.0 (M⁺ - Cl, - C₄H₇, - OMe), 618.0, 281.3 (M⁺ - MeO - MOP).

Synthesis of [PtCl(η³-C₃H₄(Me))(1b, Ar = Ph)](BARF), 16. To a mixture of H-MOP (70 mg, 0.245 mmol) and [Pt(μ-Cl)(η³-C₃H₄(Me))]₂ (70 mg, 0.123 mmol) was added 4 mL of CH₂Cl₂, and the resulting solution was stirred for 60 min at room temperature. After removal of the solvent, the pale orange product was washed with 4 mL of pentane. Yield: 158 mg (89%). Anal. Calcd for C₃₆ClH₃₀PPt: C, 59.71; H, 4.18. Found: C, 60.29; H, 4.64. ¹H NMR (CD₂Cl₂, 500 MHz, 298 K): major isomer: δ 8.12-6.69 (aromatic), 3.82 (H^{cis}-L3), 2.74 (H^{cis}-L1), 2.02 (H^{trans}-L3), 2.01 (s, CH₃-L2), 1.30 (H^{trans}-L1). Minor isomer: δ 8.12-6.69 (aromatic), 3.97 (H^{cis}-L3), 2.47 (H^{trans}-L3), 2.37 (H^{cis}-L1), 1.89 (s, CH₃-L2), 1.26 (H^{trans}-L1). ¹³C NMR (CD₂Cl₂, 125 MHz, 298 K): major isomer: δ 123.4 (C(CH₃)-L2), 66.4 (C-L3), 47.9 (C-L1), 23.5 (C(CH₃)-L2). Minor isomer: δ 123.8 (C(CH₃)-L2), 67.1 (C-L3), 48.1 (C-L1), 23.2 (C(CH₃)-L2). ³¹P NMR (CD₂Cl₂, 202 MHz, 298 K): major isomer: δ 26.6 (s, ¹J_{PtP} = 4361). Minor isomer: δ 23.1 (s, ¹J_{PtP} = 4110). ESI: 688.1 (M⁺ - Cl), 632.1 (M⁺ - Cl, - allyl), 554.1 (M⁺ - Cl, - allyl, - phenyl), 477.2 (M⁺ - Cl, - allyl, - 2 phenyl).

Synthesis of [Pt(η³-C₃H₄(Me))(1a, Ar = Ph)](BARF), 17. Complex **15** (74 mg, 0.098 mmol) and NaBARF (87 mg, 0.098 mmol) were dissolved in 4 mL of CH₂Cl₂, and the resulting solution was stirred for 60 min at room temperature. The NaCl formed was removed by filtration over Celite and the solvent evaporated in vacuo. Yield: 130 mg (84%). Anal. Calcd for C₆₉H₄₄OBf₂PPt: C, 52.39; H, 2.80. Found: C, 52.19; H, 3.07. ¹H NMR (CD₂Cl₂, 500 MHz, 298 K): major isomer: δ 8.03 (d, ³J_{HH} = 8.7, H-4), 7.81 (d, ³J_{HH} = 8.7, H-5), 6.99 (H-7), 3.48 (s, OCH₃), 3.38 (H^{cis}-L1), 2.22 (³J_{PH} = 8.3, H^{trans}-L3), 2.15 (H^{trans}-L1), 2.06 (H^{cis}-L3), 1.87 (³J_{PH} = 71.0, CH₃-L2). Minor isomer: δ 8.06 (³J_{HH} = 8.8, H-4), 7.89 (³J_{HH} = 8.8, H-5), 3.58 (s, OCH₃), 3.27 (³J_{PH} = 8.2, H^{cis}-L3), 2.99 (H^{cis}-L1), 2.21 (H^{trans}-L1), 1.30 (H^{trans}-L3), 1.16 (³J_{PH} = 68.0, CH₃-L2). ¹³C NMR (CD₂Cl₂, 125 MHz, 298 K): major isomer: δ 152.2 (C-6), 137.4 (C-2), 136.0 (C-4), 128.0 (C-3), 131.7 (C(CH₃)-L2), 117.7 (C-5), 96.1 (¹J_{PtC} = 109.2, C-1), 89.0 (C-L3), 57.2 (OCH₃), 46.8 (C-L1), 23.9 (C(CH₃)-L2). Minor isomer: δ 156.0 (C-6), 137.0 (C-4), 137.3 (C-2), 127.2 (C-3), 121.5 (C-L2), 116.3 (C-5), 95.8 (¹J_{PtC} = 106.1, C-1), 89.5 (C-L3), 57.3 (OCH₃), 45.5 (C-L1), 22.7 (C(CH₃)-L2). ³¹P NMR (CD₂Cl₂, 202 MHz, 298 K): major isomer: δ 40.0 (s, ¹J_{PtP} = 4093). Minor isomer: δ 40.1 (s, ¹J_{PtP} = 4110). ESI: 718.1 (M⁺ - Cl), 694.0, 662.0 (M⁺ - Cl, - C₄H₇), 633.0 (M⁺ - Cl, - C₄H₇, - OMe), 618.0.

Synthesis of [Pt(η³-C₃H₄(Me))(1b, Ar = Ph)](BARF), 18. [PtCl(η³-C₃H₄(Me))(H-MOP)], **16** (74 mg, 0.098 mmol), and NaBARF (87 mg, 0.098 mmol) were dissolved in 4 mL of CH₂Cl₂, and the resulting solution was stirred for 60 min at room temperature. The NaCl formed was removed by filtration and the solvent evaporated in vacuo. Dissolving the solid in Et₂O

and precipitation at $-48\text{ }^{\circ}\text{C}$ afforded a pale yellow solid. Yield: 91 mg (80%), $[\text{Pt}(\eta^3\text{-C}_3\text{H}_4(\text{Me}))(\text{H-MOP})](\text{BArF})$. Anal. Calcd for $\text{C}_{68}\text{H}_{42}\text{BF}_{24}\text{PPT}$: C, 52.63; H, 2.73. Found: C, 52.04; H, 2.86. ^1H NMR (CD_2Cl_2 , 500 MHz, 298 K): major isomer: δ 8.11 (dd, $^3J_{\text{HH}} = 5.9$ and 8.6 , H-5), 7.71 ($^3J_{\text{HH}} = 8.6$, H-4), 6.49 (d, $^3J_{\text{HH}} = 5.9$, H-6), 3.40 ($\text{H}^{\text{cis-L3}}$), 3.40 ($\text{H}^{\text{cis-L1}}$), 2.44 ($^4J_{\text{HH}} = 2.2$, $^2J_{\text{PtH}} = 73.3$, $\text{H}^{\text{trans-L1}}$), 2.25 ($^3J_{\text{PH}} = 7.9$, $\text{H}^{\text{trans-L3}}$), 1.88 (s, $^3J_{\text{PtH}} = 73.5$, $\text{CH}_3\text{-L2}$). Minor isomer: δ 8.18 (dd, $^3J_{\text{HH}} = 6.1$ and 8.6 , H-5), 7.74 ($^3J_{\text{HH}} = 8.6$, H-4), 6.57 ($^3J_{\text{HH}} = 6.1$, H-6), 3.68 ($^3J_{\text{PH}} = 9.2$, $\text{H}^{\text{cis-L3}}$), 2.99 ($\text{H}^{\text{cis-L1}}$), 2.17 ($^4J_{\text{HH}} = 3.4$, $\text{H}^{\text{trans-L1}}$), 2.02 ($\text{H}^{\text{trans-L3}}$), 1.02 (s, $^3J_{\text{PtH}} = 69.5$, $\text{CH}_3\text{-L2}$). ^{13}C NMR (CD_2Cl_2 , 125 MHz, 298 K): major isomer: δ 136.2 ($\text{C}(\text{CH}_3)\text{-L2}$), 132.8 (C-3), 132.6 (C-2), 131.9 (C-5), 129.9 (C-4), 116.1 ($^1J_{\text{PtC}} = 89.0$, C-1), 95.0 ($^1J_{\text{PtC}} = 56.1$, C-2), 89.4 (C-L3), 54.5 (C-L1), 24.2 ($\text{C}(\text{CH}_3)\text{-L2}$). Minor isomer: δ 132.8 ($\text{C}(\text{CH}_3)\text{-L2}$), 132.5 (C-5), 132.2 (C-3), 132.0 (C-2), 129.7 (C-4), 118.7 ($^1J_{\text{PtC}} = 76.0$, C-1), 96.1 ($^1J_{\text{PtC}} = 48.6$, C-2), 92.4 (C-L3), 49.4 (C-L1), 23.0 ($\text{C}(\text{CH}_3)\text{-L2}$). ^{31}P NMR (CD_2Cl_2 , 202 MHz, 298 K): major isomer: δ 35.8 (s, $^1J_{\text{PtP}} = 4075$) isomer: δ 36.2 (s, $^1J_{\text{PtP}} =$

4071). ESI: 688.1 (M^+), 631.9 ($\text{M}^+ - \text{allyl}$), 554.9 ($\text{M}^+ - \text{allyl}$, $- \text{phenyl}$), 478.0 ($\text{M}^+ - \text{allyl}$, $- 2 \text{ phenyl}$).

Acknowledgment. P.S.P. thanks the Swiss National Science Foundation and the ETH Zurich for financial support. A.A. thanks M.I.U.R. for a research grant (PRIN 2002). We also thank Johnson Matthey, U.K., for the loan of precious metal salts.

Supporting Information Available: Text giving experimental details and a full listing of crystallographic data for **13**, including tables of positional and isotropic equivalent displacement parameters, anisotropic displacement parameters, calculated positions of the hydrogen atoms, bond distances, and bond angles. ORTEP figure showing the full numbering schemes. X-ray data are also available as a CIF file. This material is available free of charge via the Internet at <http://pubs.acs.org>.

OM049039T